

Stochastic MPC with Multi-modal Predictions for Traffic Intersections

Siddharth H. Nair*, Vijay Govindarajan*, Theresa Lin, Chris Meissen, H. Eric Tseng, Francesco Borrelli

Abstract—We propose a Stochastic MPC (SMPC) formulation for autonomous driving at traffic intersections which incorporates multi-modal predictions of surrounding vehicles for collision avoidance constraints. The multi-modal predictions are obtained with Gaussian Mixture Models (GMM) and constraints are formulated as chance-constraints. Our main theoretical contribution is a SMPC formulation that optimizes over a novel feedback policy class designed to exploit additional structure in the GMM predictions, and that is amenable to convex programming. The use of feedback policies for prediction is motivated by the need for reduced conservatism in handling multi-modal predictions of the surrounding vehicles, especially prevalent in traffic intersection scenarios. We evaluate our algorithm along axes of mobility, comfort, conservatism and computational efficiency at a simulated intersection in CARLA. Our simulations use a kinematic bicycle model and multimodal predictions trained on a subset of the Lyft Level 5 prediction dataset. To demonstrate the impact of optimizing over feedback policies, we compare our algorithm with two SMPC baselines that handle multi-modal collision avoidance chance constraints by optimizing over open-loop sequences.

I. INTRODUCTION

Motivation

Autonomous vehicle technologies have seen a surge in popularity over the last decade, with the potential to improve flow of traffic, safety and fuel efficiency [1]. While existing technology is being gradually introduced into scenarios such as highway driving and low-speed parking, the traffic intersection scenario presents a complex challenge, especially in the absence of vehicle-to-vehicle communication. In any traffic scenario, an autonomous vehicle agent must plan to follow its desired route while accounting for surrounding agents to maintain safety. The difficulty arises from the variability in the possible behaviors of the surrounding agents [2], [3]. To address this difficulty, significant research has been devoted to modelling these agent predictions as multi-modal distributions [4], [5], [6]. Such models capture uncertainty in both high-level decisions (desired route) and low-level executions (agent position, heading, speed).

The focus of this work is to investigate how to incorporate these multi-modal distributions for the surrounding agents (target vehicles) into a planning framework for the autonomous agent (ego vehicle). The main challenge in designing such a framework is to find a good balance between performance, safety, and computation time. We investigate this planning problem in the context of constrained optimal

control and use Model Predictive Control (MPC), the state-of-the-art for real-time optimal control [7], [8]. We assume that predictions of the other agents are specified as Gaussian Mixture Models (GMMs) and propose a Stochastic Model Predictive Control (SMPC) framework that incorporates probabilistic collision avoidance and actuation constraints.

Related work

There is a large body of work focusing on the application of SMPC to autonomous driving [9], [10]. A typical SMPC algorithm involves solving a chance-constrained finite horizon optimal control problem in a receding horizon fashion [11]. The chance-constrained SMPC optimization problem, offers a less conservative modelling framework for handling constraints in uncertain environments compared to Robust MPC frameworks. In the context of autonomous driving, SMPC has been used for imposing chance constraints accounting for uncertainty in both the ego vehicle and target vehicle predictions in applications such as autonomous lane change [12], [13], cruise control [14] and platooning [15]. A common feature of works in these applications is that the predictions are either uni-modal or the underlying mode of the multi-modal prediction can be inferred accurately.

In order to handle multi-modal predictions (specifically GMMs), the work in [16] and [17] proposes nonlinear SMPC algorithms that suitably reformulate the collision avoidance chance constraint for all possible modes and demonstrate their algorithms at traffic intersection scenarios. However, a non-convex optimization problem is formulated to find a single open-loop input sequence that satisfies the collision avoidance chance constraints for all modes and possible evolutions of the target vehicles over the prediction horizon given by the GMM. This approach can be conservative and a feasible solution to the optimization problem may not exist. To remedy this issue, we optimize over a class of feedback policies [18] which adds flexibility due to the ability to react to realizations of the ego and target vehicle trajectories along the prediction horizon.

The work in [19] and [20] is the closest to our approach. The former considers uni-modal predictions and fixes a policy (computed offline) for which the optimization problem can still be conservative. The latter proposes a Robust MPC scheme that optimizes over policies with known, bounded polytopic supports for multi-modal distributions of the obstacle. However, this is done by enumerating over all possible sequences of vertices of the support of the obstacle distribution, resulting in a formulation where the number of constraints is exponential in the prediction horizon.

*Indicates equal contribution. SHN, VG and FB are with the Model Predictive Control Laboratory, UC Berkeley. TL and CM are with Ford AV LLC. HET is with Ford Research and Advanced Engineering. {siddharth_nair, govvijay, fborrelli}@berkeley.edu and {tlin33, cmeissen, htseng}@ford.com.

Contributions

Our main contributions are summarised as follows:

- We propose a SMPC framework that optimizes over a novel class of feedback policies designed to exploit additional structure in the GMM predictions. These policies assume feedback over the ego vehicle state and the target vehicle positions, thus reducing conservatism. Moreover, we show that our SMPC optimization problem can be posed as a Second-Order Cone Program (SOCP).
- We present a systematic evaluation of our framework along axes of (i) mobility, (ii) comfort, (iii) conservatism and (iv) computational efficiency at a simulated traffic intersection. To demonstrate the impact of optimizing over feedback policies, we include two baselines: (i) a chance-constrained Nonlinear MPC optimizing over open-loop sequences with the multi-modal collision avoidance chance-constraints as in [17] and (ii) an ablation of our SMPC formulation, which optimizes over open-loop sequences instead of feedback policies.

In the interest of space, we defer proofs and extensive simulation results to our website¹.

II. PROBLEM FORMULATION

In this section we formally cast the problem of designing SMPC in the context of autonomous driving at intersections.

A. Preliminaries

Notation: The index set $\{k_1, k_1 + 1, \dots, k_2\}$ is denoted by $\mathcal{I}_{k_1}^{k_2}$. Given random variables X and Y , we write $X|Y$ as a shorthand for $X|Y = y$ (X conditioned on $Y = y$). Given a normal distribution $\mathcal{N}(\mu, \Sigma)$ and $\beta \geq 0$, define the β -confidence ellipsoid $\mathcal{E}(\mu, \Sigma, \beta) = \{x : (x - \mu)^\top \Sigma^{-1} (x - \mu) \leq \beta\}$. For any two positive semi-definite matrices $M_1, M_2 \in \mathbb{S}_+^n$, we have $M_1 \prec M_2 \Leftrightarrow M_2 - M_1 \in \mathbb{S}_+^n$. The binary operator \otimes denotes the Kronecker product. The partial derivative of function $f(x, u)$ with respect to x at $(x, u) = (x_0, u_0)$ is denoted by $\partial_x f(x_0, u_0)$.



Fig. 1: Depiction of an unsignalized intersection with green Ego Vehicle (EV) and orange Target Vehicle (TV). The EV arrives first and intends to turn left (green path). The EV is provided 3 possible predictions of TV behavior in decreasing order of probability (red: give EV right-of-way, orange: turn left and yellow: go straight).

Intersection setup: Consider the intersection shown in Figure 1. The Ego Vehicle (EV), depicted in green, is the vehicle to be controlled. All other vehicles at the intersection are called Target Vehicles (TVs).

EV modeling: Let $x_t = [X_t \ Y_t \ \theta_t \ v_t]^\top$ be the state of the EV at time t with (X_t, Y_t) and θ_t being its position and heading respectively in global coordinates, and v_t being its speed. The discrete-time dynamics of the EV are given by the Euler discretization of the kinematic bicycle model [21], denoted as $x_{t+1} = f^{EV}(x_t, u_t)$. The control inputs $u_t = [a_t \ \delta_t]^\top$ are the acceleration a_t and front steering angle δ_t . The system state and input constraints are given by polytopic sets \mathcal{X}, \mathcal{U} respectively.

As depicted by the green path in Figure 1, we assume a kinematically feasible reference trajectory,

$$\{(x_t^{ref}, u_t^{ref})\}_{t=0}^T \quad (1)$$

is provided for the EV. This serves as the EV's desired trajectory which can be computed offline (or online at low frequency) by solving a nonlinear trajectory optimization problem, while accounting for the EV's route, actuation limits, and static environment constraints (like lane boundaries, traffic rules). However, this reference does not consider the dynamically evolving TVs for real-time obstacle avoidance.

TV predictions: We focus our presentation on a single TV although the proposed framework can be generalised for multiple TVs. Let $o_t = [X_t^o \ Y_t^o]^\top$ be the position (and state) of the TV at time t . For the purpose of dynamic obstacle avoidance, we assume that we are provided predictions of the TV's position for N time steps in the future, given by the random variables $\{o_{k|t}\}_{k=1}^N$, where each random variable $o_{k|t}$ describes the position of the TV at time $t+k$ conditioned on the current position o_t . The predictions for the TV at time t is encoded as a Gaussian Mixture Model (GMM):

$$\mathcal{G}_t = \left\{ p_{t,j}, \{\mathcal{N}(\mu_{k|t,j}, \Sigma_{k|t,j})\}_{k=1}^N \right\}_{j=1}^J \quad (2)$$

where

- J is the number of possible modes.
- $\mathbb{P}(\sigma_t = j | o_t) = p_{t,j} \in [0, 1]$ is the probability that the mode at time t , denoted by σ_t , is j for some $j \in \mathcal{I}_1^J$.
- $o_{k|t,j} \sim \mathcal{N}(\mu_{k|t,j}, \Sigma_{k|t,j})$, i.e., the position of the TV at time $t+k$ conditioned on the current position o_t and mode $\sigma_t = j$, denoted by $o_{k|t,j}$, is given by the Gaussian distribution $\mathcal{N}(\mu_{k|t,j}, \Sigma_{k|t,j})$.

The multi-modal distribution of $o_{k|t}$ is thus given by

$$o_{k|t} \sim \sum_{j=1}^J p_{t,j} \mathcal{N}(\mu_{k|t,j}, \Sigma_{k|t,j}) \quad \forall k \in \mathcal{I}_1^N. \quad (3)$$

B. Qualitative Control Objectives

- Design a feedback control $u_t = \pi_t(x_t, o_t)$ for the EV to track the reference trajectory (1) while avoiding collisions with the TV, whose predictions are given by the GMM (2).
- The algorithm to compute u_t must be computationally tractable and not overly conservative.

¹Supplementary material, videos, code @ [Project Website](#)

C. Overview of Proposed Approach

We propose a novel SMPC formulation to compute the feedback control u_t . The optimization problem of our SMPC takes the form,

$$\min_{\mathbf{u}_t, \mathbf{x}_t, \mathbf{o}_t} J_t(\mathbf{x}_t, \mathbf{u}_t) \quad (4a)$$

$$\text{s.t.} \quad x_{k+1|t} = f_k^{EV}(x_{k|t}, u_{k|t}), \quad (4b)$$

$$o_{k+1|t}|o_{k|t} \sim f_k^{TV}(o_{k|t}), \quad (4c)$$

$$\mathbb{P}(g_k(o_{k+1|t}, x_{k+1|t}) \leq 0) \leq \epsilon, \quad (4d)$$

$$(x_{k+1|t}, u_{k|t}) \in \mathcal{X} \times \mathcal{U}, \quad (4e)$$

$$\mathbf{u}_t \in \Pi(\mathbf{x}_t, \mathbf{o}_t), \quad (4f)$$

$$x_{0|t} = x_t, \quad o_{0|t} = o_t, \quad (4g)$$

$$\forall k \in \mathcal{I}_0^{N-1}$$

where $\mathbf{u}_t = [u_{0|t}, \dots, u_{N-1|t}]$, $\mathbf{x}_t = [x_{0|t}, \dots, x_{N|t}]$ and $\mathbf{o}_t = [o_{0|t}, \dots, o_{N|t}]$. The SMPC feedback control action is given by the optimal solution of (4) as

$$u_t = \pi_{\text{SMPC}}(x_t, o_t) = u_{0|t}^* \quad (5)$$

where the EV and TV state feedback enters as (4g).

The objective (4a) penalizes deviation of the EV trajectory from the reference (1) and the collision avoidance constraints are imposed as chance constraints (4d) along with polytopic state and input constraints \mathcal{X}, \mathcal{U} for the EV. The TV predictions in (4c) are obtained from the GMM (2) and assuming additional dynamical structure (discussed in Sec. III-B). Using this, our SMPC optimizes over a novel policy class (4f) that depends on predictions of the EV's and TV's states as opposed to optimization over open-loop sequences which can often be conservative. This is our main theoretical contribution. Moreover, we show that (4) can be posed as a convex optimization problem, making it computationally tractable and amenable to state-of-the-art solvers. This is achieved by (i) a convex parameterisation of policy class $\Pi(\cdot)$, (ii) using affine time varying models to generate EV and TV state predictions in (4b) and (4c), (iii) using a convex cost function for (4a), and (iv) constructing convex inner approximations of (4d).

III. STOCHASTIC MPC WITH MULTI-MODAL PREDICTIONS

In this section, we detail our SMPC formulation for the EV to track the reference (1) while incorporating multi-modal predictions from (2) of the TV for obstacle avoidance.

A. EV prediction model

The EV prediction model (4b) is a linear time-varying model, obtained by linearizing $f^{EV}(\cdot)$ about the reference trajectory (1). Defining $x_{k|t} - x_{t+k}^{ref} = \Delta x_{k|t}$ and $u_{k|t} - u_{t+k}^{ref} = \Delta u_{k|t}$, we have $\forall k \in \mathcal{I}_0^{N-1}$,

$$\Delta x_{k+1|t} = A_{k|t} \Delta x_{k|t} + B_{k|t} \Delta u_{k|t} + w_{k|t} \quad (6)$$

$$A_{k|t} = \partial_x f^{EV}(x_{t+k}^{ref}, u_{t+k}^{ref}), \quad B_{k|t} = \partial_u f^{EV}(x_{t+k}^{ref}, u_{t+k}^{ref})$$

where the additive process noise $w_{k|t} \sim \mathcal{N}(0, \Sigma_w)$ (i.i.d with respect to k) models linearization error and other stochastic

noise sources. Consequently, the polytopic state and input constraints (4e) are then written as chance constraints $\forall k \in \mathcal{I}_0^{N-1}$,

$$\mathbb{P}((\Delta x_{k+1|t}, \Delta u_{k|t}) \in \Delta \mathcal{X}_k \times \Delta \mathcal{U}_k) \geq 1 - \epsilon \quad (7)$$

$$\Delta \mathcal{X}_k = \{\Delta x : F_k^x \Delta x \leq f_k^x\}, \quad \Delta \mathcal{U}_k = \{\Delta u : F_k^u \Delta u \leq f_k^u\}.$$

B. TV prediction model

Notice that the multi-modal distribution of the random variable $o_{k+1|t}$ (as given by (3)) is independent of the random variable $o_{k|t}$, i.e., $o_{k+1|t}|o_{k|t} = o_{k+1|t}$. However, since the TV positions are governed by the laws of motion, it is reasonable to assume dynamical structure to link positions at consecutive time steps such that $o_{k+1|t}|o_{k|t} \neq o_{k+1|t}$. Thus, a measurement of $o_{k|t}$ reduces the uncertainty in $o_{k+1|t}$, which can be exploited by the policy class (4f) in the SMPC problem. We model this structure using affine time-varying models for each mode, constructed using the parameters of the GMM (2) as follows.

We assume $\forall k \in \mathcal{I}_0^{N-1}, \forall j \in \mathcal{I}_1^J$ that $o_{k+1|t,j}$ conditioned on $o_{k|t,j}$ is given by the distribution

$$o_{k+1|t,j}|o_{k|t,j} \sim \mathcal{N}(T_{k|t,j} o_{k|t,j} + c_{k|t,j}, \tilde{\Sigma}_{k+1|t,j}), \quad (8)$$

where $\forall k \in \mathcal{I}_1^{N-1}$,

$$T_{k|t,j} = \sqrt{\Sigma_{k+1|t,j}} \sqrt{\Sigma_{k|t,j}^{-1}}, \quad c_{k|t,j} = \mu_{k+1|t,j} - T_{k|t,j} \mu_{k|t,j},$$

$$\tilde{\Sigma}_{k+1|t,j} = \Sigma_n \quad (\text{for some } \Sigma_n \prec \Sigma_{k+1|t,j}, \Sigma_n \succ 0) \quad (9)$$

and $T_{0|t,j} = I$, $c_{0|t,j} = \mu_{1|t,j} - o_t$, $\tilde{\Sigma}_{1|t,j} = \Sigma_{1|t,j}$. For $k \geq 1$, this model captures the notion that if $o_{k|t,j}$ is S standard deviations away from $\mu_{k|t,j}$, then $o_{k+1|t,j}$ will also be about S standard deviations away from $\mu_{k+1|t,j}$. To justify our construction of $\{\{T_{k|t,j}, c_{k|t,j}, \tilde{\Sigma}_{k+1|t,j}\}_{k=0}^{N-1}\}_{j=1}^J$, we compute the distribution of $o_{k|t,j}$ using (8) in the next proposition, and compare it to the distribution of $o_{k|t,j}$ obtained directly from the GMM (2).

Proposition 1: Given $\sigma_t = j \in \mathcal{I}_1^J$ and $o_{0|t,j} = o_t$, we have for any $k \in \mathcal{I}_1^N$ using (8) (constructed from \mathcal{G}_t using (9)) that

$$o_{k|t,j} \sim \mathcal{N}(\mu_{k|t,j}, \Sigma_{k|t,j} + \Sigma_n + \bar{\Sigma}_{k|t,j})$$

where $\bar{\Sigma}_{k|t,j} = \sum_{m=1}^{k-2} \sqrt{\Sigma_{k-1|t,j} \Sigma_{m|t,j}^{-1}} \Sigma_n \sqrt{\Sigma_{k-1|t,j} \Sigma_{m|t,j}^{-1}}$.

Proof: Appendix B¹. ■

Thus with our assumed model (8), the distribution of $o_{k|t,j}$ has the same mean as given by the GMM (2) but with an increase in variance by $\Sigma_n + \bar{\Sigma}_{k|t,j}$.

The model in (8) describes inference over the state of the TV by conditioning the observations of the TV states on a given mode $\sigma_t = j$. To complete the description of the TV's multi-modal predictions, we now discuss inference over the mode σ_t using observations $o_{k|t}$. There are sophisticated methods for computing the posterior probability distribution $\mathbb{P}(\sigma_t = j|o_{k|t}) = p_{k|t,j}$ (e.g. using Bayes' rule or E-M for inference on state and mode) but these would complicate our SMPC optimization problem (4). Instead, we assume $p_{k|t,j} = p_{t,j} \forall k < \bar{k}$ and at some \bar{k} , the mode can be exactly inferred from the TV's state. Motivated by [20], our model for determining \bar{k} is given by

$$\min \{k \in \mathcal{I}_1^N : \mathcal{E}(\mu_{l|t,j_1}, \Sigma_{l|t,j_1}, \beta) \cap \mathcal{E}(\mu_{l|t,j_2}, \Sigma_{l|t,j_2}, \beta) = \emptyset, \forall l \geq k, \forall j_1, j_2 \in \mathcal{I}_1^J\} \quad (10)$$

Thus \bar{k} is the minimum time step along the prediction horizon such that all β -confidence ellipsoids for subsequent time steps are pairwise disjoint for all modes. Given k , we assume that the mode of the i th TV can be determined using state $o_{\bar{k}|t}$ as given by

$$p_{\bar{k}|t,j} = \begin{cases} 1 & \text{if } o_{\bar{k}|t} \in \mathcal{E}(\mu_{k|t,j}, \Sigma_{k|t,j}, \beta) \\ 0 & \text{otherwise} \end{cases} \quad (11)$$

and $p_{k|t,j} = p_{\bar{k}|t,j} \forall k \in \mathcal{I}_k^{N-1}$. In summary, we use (8) and (11) to obtain the TV prediction model $f_k^{TV}(\cdot)$ in (4c) as the multi-modal distribution of $o_{k+1|t}$ conditioned on $o_{k|t}$,

$$o_{k+1|t}|o_{k|t} \sim \sum_{j=1}^J p_{k|t,j} \mathcal{N}(T_{k|t,j} o_{k|t} + c_{k|t,j}, \tilde{\Sigma}_{k+1|t,j}). \quad (12)$$

Defining $n_{k|t,j} \sim \mathcal{N}(0, \tilde{\Sigma}_{k+1|t,j}) \forall k \in \mathcal{I}_0^{N-1}, \forall j \in \mathcal{I}_1^J$, we can use properties of Gaussian random variables (closure under linear combinations and the orthogonality principle) to rewrite (12) as

$$o_{k+1|t} = T_{k|t,\sigma_t} o_{k|t} + c_{k|t,\sigma_t} + n_{k,\sigma_t} \quad \forall k \in \mathcal{I}_0^{N-1} \quad (13)$$

where the posterior distributions of the mode σ_t are determined using

$$\sigma_t|o_{k|t} = \begin{cases} \sigma_t & \forall k < \bar{k} \\ \sigma_t|o_{\bar{k}|t} \text{ given by (11)} & \forall k \geq \bar{k} \end{cases}. \quad (14)$$

C. Multi-modal Collision Avoidance Constraints

We assume that we are given or can infer the TV rotation matrices for each mode along the prediction horizon as $\{\{R_{k|t,j}\}_{k=1}^N\}_{j=1}^J$. For collision avoidance between the EV and the TV, we impose the following chance constraint

$$\mathbb{P}(g_{k|t}(P_{k|t}, o_{k|t}) \geq 1) \geq 1 - \epsilon \quad \forall k \in \mathcal{I}_1^N \quad (15)$$

where $P_{k|t} = [\Delta X_{k|t} \ \Delta Y_{k|t}]^\top + P_{k|t}^{ref}$ with $P_{k|t}^{ref} = [X_{t+k}^{ref} \ Y_{t+k}^{ref}]^\top$ given by (1), $[\Delta X_{k|t} \ \Delta Y_{k|t}]^\top$ given by (6), and

$$g_{k|t}(P, o) = (P - o)^\top R_{k|t,\sigma_t}^\top \begin{bmatrix} \frac{1}{a_{ca}^2} & 0 \\ 0 & \frac{1}{b_{ca}^2} \end{bmatrix} R_{k|t,\sigma_t} (P - o). \quad (16)$$

$a_{ca} = a_{TV} + d_{EV}$, $b_{ca} = b_{TV} + d_{EV}$ are semi-axes of the ellipse containing the TV's extent with a buffer of d_{EV} . $g_{k|t}(P, o) \geq 1$ implies that the EV's extent (modelled as a disc of radius d_{EV} and centre P) does not intersect the TV's extent (modelled as an ellipse with semi-axes a_{TV} , b_{TV} and centre o , oriented as given by $R_{k|t,\sigma_t}$). This constraint is non-convex because it involves the integral of the nonlinear function $g_{k|t}(\cdot)$ over the joint distribution of $(P_{k|t}, o_{k|t}, \sigma_t)$. To address the multi-modality, we conservatively impose the chance constraint conditioned on every mode with the same risk level $1 - \epsilon$ because of the following implication

$$\begin{aligned} \mathbb{P}(g_{k|t,j}(P_{k|t}, o_{k|t,j}) \geq 1) &\geq 1 - \epsilon \quad \forall j \in \mathcal{I}_1^J \\ \Rightarrow \mathbb{P}(g_{k|t}(P_{k|t}, o_{k|t}) \geq 1) &\geq 1 - \epsilon \end{aligned}$$

where $g_{k|t,j}(P, o)$ is defined by conditioning (16) on mode j . To address the nonlinearity, we use the convexity of $g_{k|t,j}(\cdot)$ to construct its linear under-approximation in the following proposition.

Proposition 2: For collision avoidance, define EV positions $\forall k \in \mathcal{I}_1^N, \forall j \in \mathcal{I}_1^J$ as $P_{k|t,j}^{ca} = \mu_{k|t,j} +$

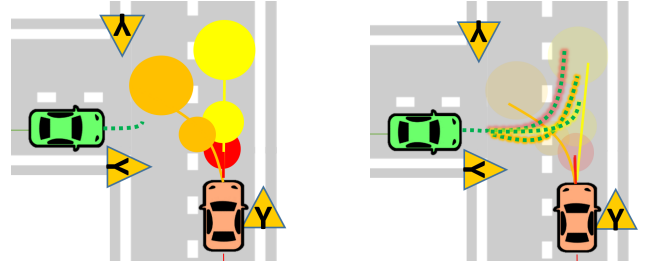
$\frac{1}{\sqrt{g_{k|t,j}(P_{k|t}^{ref}, \mu_{k|t,j})}} (P_{k|t}^{ref} - \mu_{k|t,j})$. Then for the affine function, $g_{k|t,j}^L(P, o) = \partial_P g_{k|t}(P_{k|t,j}^{ca}, \mu_{k|t,j})(P - P_{k|t,j}^{ca}) + \partial_o g_{k|t}(P_{k|t,j}^{ca}, \mu_{k|t,j})(o - \mu_{k|t,j})$, we have $\forall k \in \mathcal{I}_0^{N-1}$

$$\begin{aligned} \mathbb{P}(g_{k+1|t,j}^L(P_{k+1|t}, o_{k+1|t,j}) \geq 0) &\geq 1 - \epsilon \quad \forall j \in \mathcal{I}_1^J \quad (17) \\ \Rightarrow \mathbb{P}(g_{k|t}(P_{k+1|t}, o_{k+1|t}) \geq 1) &\geq 1 - \epsilon \end{aligned}$$

Proof: Appendix C¹. ■

We build on these approximations to complete the reformulation of (15) for EV and TV trajectories given by (6), (13) in closed-loop with a feedback policy.

D. Predictions using EV and TV state feedback policies



(a) Prediction with open-loop sequences $\mathbf{u}_t \in \mathbb{R}^{2 \times N}$

(b) Predictions with policies $\mathbf{u}_t \in \Pi(\mathbf{x}_t, \mathbf{o}_t)$

Fig. 2: In (a), solving (4) over open-loop sequences can be conservative because EV prediction (green-dashed) from a single sequence of control inputs must satisfy all the obstacle avoidance constraints. In (b), optimizing over policies (4f) allows for different EV predictions depending on the TV trajectory realizations (green-dashed with highlights corresponding to different TV trajectories).

We present a policy class, $\Pi(\mathbf{x}_t, \mathbf{o}_t)$, for the EV that accounts for state feedback from both the EV and TVs. In general, optimizing over state feedback policies subsumes optimizing over open-loop sequences in (4) because the former has a strictly larger feasible set. For the assumed EV model (6) and mode-dependent TV model (13), we propose the following feedback policy for the EV:

$$\Delta u_{k|t} = \pi_{k|t}(x_{k|t}, o_{k|t}) = \begin{cases} h_{k|t} + \sum_{l=0}^{k-1} M_{l,k|t} w_{l|t} + K_{k|t} o_{k|t} & \text{if } k < \bar{k} \\ h_{k|t}^1 + \sum_{l=0}^{k-1} M_{l,k|t}^1 w_{l|t} + K_{k|t}^1 o_{k|t} & \text{if } k \geq \bar{k}, \sigma_t = 1 \\ \vdots & \vdots \\ h_{k|t}^J + \sum_{l=0}^{k-1} M_{l,k|t}^J w_{l|t} + K_{k|t}^J o_{k|t} & \text{if } k \geq \bar{k}, \sigma_t = J \end{cases}. \quad (18)$$

This policy uses affine disturbance feedback for feedback over EV states (c.f. [18] for proof of equivalence) and linear feedback over TV states. Moreover since the mode of the TV can be determined as given by (14), we use separate mode-dependent policies along the prediction horizon for $k \geq \bar{k}$. For each $j \in \mathcal{I}_1^J$, denote the policy parameterization in (18) by $\mathbf{h}_t^j \in \mathbb{R}^{2N}$, $\mathbf{M}_t^j \in \mathbb{R}^{2N \times 4N}$, $\mathbf{K}_t^j \in \mathbb{R}^{2N \times 2N}$ (see Appendix A¹ for definitions). Given x_t and o_t , define the following set of policy parameters of (18) that satisfy the EV state and input chance constraints (7) and the multi-modal

collision avoidance chance constraint (17):

$$\Pi_t(x_t, o_t) = \left\{ \begin{array}{l} \{\mathbf{h}_t^j, \mathbf{M}_t^j, \mathbf{K}_t^j\}_{j=1}^J \quad (7), (17) \text{ hold } \forall k \in \mathcal{I}_0^{N-1}, \\ \Delta x_{0|t} = x_t - x_t^{ref}, o_{0|t} = o_t \end{array} \right\} \quad (19)$$

Proposition 3: Let $\epsilon < \frac{1}{2}$. Then the set of policy parameters $\Pi_t(x_t, o_t)$ is a Second-Order Cone (SOC).

Proof: Appendix D¹. ■

E. SMPC Optimization Problem

We define the cost (4a) of the SMPC optimization problem (4) to penalise deviations of the EV state and input trajectories from the reference trajectory (1) as

$$J_t(\mathbf{x}_t, \mathbf{u}_t) = \mathbb{E} \left(\sum_{k=0}^{N-1} \Delta x_{k+1|t}^T Q \Delta x_{k+1|t} + \Delta u_{k|t}^T R \Delta u_{k|t} \right) \quad (20)$$

where $Q \succ 0, R \succ 0$. With this cost definition, we obtain the EV control (5) from our SMPC formulation as:

$$\min_{\{\mathbf{h}_t^j, \mathbf{K}_t^j, \mathbf{M}_t^j\}_{j=1}^J \in \Pi_t(x_t, o_t)} J_t(\mathbf{x}_t, \mathbf{u}_t).$$

The next proposition characterises this optimization problem.

Proposition 4: The SMPC control action (5) is given by solving the following Second-Order Cone Program (SOCP):

$$\begin{array}{ll} \min & s \\ \text{s.t. } & \{\mathbf{h}_t^j, \mathbf{K}_t^j, \mathbf{M}_t^j\}_{j=1}^J \\ & \{\mathbf{h}_t^j, \mathbf{K}_t^j, \mathbf{M}_t^j\}_{j=1}^J \in \Pi_t(x_t, o_t), \\ & N_t(\{\mathbf{h}_t^j, \mathbf{K}_t^j, \mathbf{M}_t^j\}_{j=1}^J) \leq s + r_t \end{array} \quad (21)$$

where $N_t(\cdot)$ is convex and quadratic in $\{\mathbf{h}_t^j, \mathbf{K}_t^j, \mathbf{M}_t^j\}_{j=1}^J$ and r_t is a constant determined by x_t , the EV reference trajectory (1) and the process noise covariance Σ_w .

Proof: Appendix E¹. ■

IV. EXPERIMENTAL DESIGN

In order to assess the benefits of our proposed stochastic MPC formulation, we use the CARLA [22] simulator to run closed-loop simulations¹. In this section, we describe the simulation environment, evaluated scenarios, and prediction framework used to generate multimodal predictions. We then show how the stochastic MPC formulation is integrated into a planning framework to address these multimodal predictions. Finally, we provide a set of metrics and baseline policies used to evaluate the performance of our approach.

A. CARLA Simulation Environment

The EV is tasked with passing through the intersection depicted in Figure 3, while avoiding any TVs simultaneously driving through the same intersection. The scenarios are:

- 1) EV turns left while TV drives straight.
- 2) EV turns right while TV turns left into the same road segment.
- 3) EV turns left while TV turns left into the opposite road segment.

To ensure improved repeatability of our experiments, we use the synchronous mode of CARLA. This ensures that all processing (prediction, planning, and control) is complete

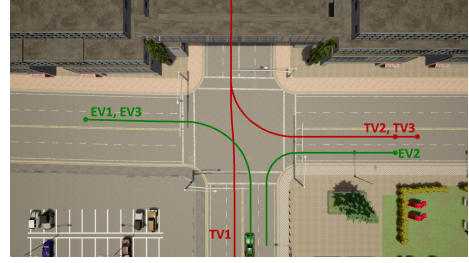


Fig. 3: Routes used for EV and TV vehicles with the scenario indicated by the numeric label. The EV follows a green path, while the TV follows a red path with the same scenario index.

before advancing the simulation. Thus, our results only consider the impact of the control inputs selected and not the time delays incurred in computing them².

The control for the TV is described by a simple nonlinear MPC (NMPC) scheme to track a pre-specified reference. For realism, the TV's NMPC also uses short predictions of the EV for simple distance-based obstacle avoidance constraints. Additionally, we note that while the intersection has traffic lights, these are ignored in our experiments. Effectively, each scenario is treated as an interaction at an unsignalized intersection.

B. Multimodal Prediction Architecture

A key assumption in our stochastic MPC approach is that the target vehicle's future motion is described by a GMM (2). To generate this probability distribution, we implement a variant of the MultiPath prediction model proposed in [5]. The input to this neural network architecture is a semantic image and pose history for the target vehicle in the scene. These inputs are used to generate a GMM over future trajectories by regression with respect to a set of predetermined anchors and classification over the anchor probabilities. We note, however, that our SMPC approach is appropriate for any prediction model that produces a GMM trajectory distribution.

To train the model, we selected a subset of the Lyft Level 5 prediction dataset [23] with 16 anchor trajectories identified using k-means clustering. At runtime, we opted to truncate the GMM produced by MultiPath. In particular, we pick the top $J = 3$ modes and renormalize the mode probabilities correspondingly.

C. Motion Planning Architecture

Given the predicted multimodal distribution for the target vehicle, we use the framework introduced in Section III to generate feedback control policies for deployment.

In addition to predictions of the target vehicles, a dynamically feasible ego reference trajectory (1) must be provided. In our work, a NMPC problem is solved using IPOPT [24] which tracks a high-level route provided by the CARLA waypoint API, while incorporating dynamic and actuation constraints.

²All experiments were run on a computer with a Intel i9-9900K CPU, 32 GB RAM, and a RTX 2080 Ti GPU.

TABLE I: Closed-loop performance comparison across all scenarios.

| Scenario | Policy | Mobility | Comfort | | | Conservatism | | | Efficiency |
|----------|---------|---------------------|-------------------|----------------------------------|---------------------------------|------------------|---------------------|-------------------|------------------------|
| | | $\bar{T}_{episode}$ | \tilde{A}_{lat} | $\bar{J}_{long} (\frac{m}{s^3})$ | $\bar{J}_{lat} (\frac{m}{s^3})$ | $\Delta\tau$ (m) | \bar{d}_{min} (m) | \mathcal{F} (%) | \bar{T}_{solve} (ms) |
| 1 | SMPC_BL | 1.099 | 1.830 | 7.336 | 12.824 | 5.396 | 5.270 | 98.66 | 33.063 |
| | SMPC_OL | 1.096 | 2.113 | 2.072 | 10.746 | 3.790 | 4.848 | 100.00 | 1.600 |
| | SMPC | 1.232 | 1.217 | 2.098 | 6.554 | 1.242 | 3.578 | 100.00 | 62.399 |
| 2 | SMPC_BL | 1.366 | 1.712 | 12.334 | 6.016 | 1.130 | 10.174 | 78.59 | 44.280 |
| | SMPC_OL | 1.571 | 1.553 | 7.929 | 5.557 | 3.900 | 9.288 | 78.01 | 1.676 |
| | SMPC | 1.294 | 1.012 | 2.531 | 5.691 | 1.027 | 7.884 | 100.00 | 63.949 |
| 3 | SMPC_BL | 1.370 | 1.620 | 10.971 | 4.378 | 2.707 | 11.582 | 83.09 | 43.372 |
| | SMPC_OL | 1.211 | 1.878 | 3.944 | 8.247 | 1.603 | 11.962 | 93.07 | 1.641 |
| | SMPC | 1.152 | 1.159 | 2.143 | 8.595 | 0.734 | 7.917 | 100.00 | 61.400 |

Given the EV reference (1) and TV predictions (2), the SMPC optimization problem (21) is solved using Gurobi [25] to compute feedback control (5). When an infeasible problem is encountered, a braking control is commanded. The corresponding control action $u_{0|t}^*$ is given as a reference to a low-level control module that sets the vehicle’s steering, throttle, and brake inputs. These loops are repeated until all vehicles in the scenario reach their destination.

D. Policies

We evaluate the following set of policies:

- **SMPC**: Our proposed framework, given by solving (21) which optimizes over our policy class (19).
- **SMPC_OL**: This model is an ablation of our approach, where $\mathbf{u}_t \in \mathbb{R}^{2 \times N}$ replaces (4f) and the GMM (2) is used directly in (4c) instead of (12).
- **SMPC_BL**: Based off [17], a nonlinear SMPC algorithm is used with the collision avoidance chance constraints (4d) reformulated using VP concentration bounds. The optimization is performed over open-loop sequences, i.e., $\mathbf{u}_t \in \mathbb{R}^{2 \times N}$ instead of (4f), and no additional dynamical structure assumed as in (4c), i.e., $o_{k+1|t} \sim f_k^{TV}(o_t)$.

E. Evaluation Metrics

To evaluate the performance of our approach with respect to the baseline policies, we introduce a set of closed-loop behavior metrics. A desirable planning framework enables high mobility without being overly conservative, allowing the timely completion of the driving task, while maintaining passenger comfort. The computation time should also not be exorbitant to allow for real-time processing of updated scene information.

The following metrics are used to assess these factors:

- **Mobility**: We record the time the EV takes to reach its goal: $\bar{T}_{episode}$, normalised by the time taken to reach the same goal without target vehicles.
- **Comfort**: We record (1) the peak lateral acceleration: \tilde{A}_{lat} , normalised by the peak lateral acceleration in the absence of TVs, (2) the average longitudinal jerk: \bar{J}_{long} and (3) the average lateral jerk: \bar{J}_{lat} . High values are undesirable, linked to sudden braking or steering.
- **Conservatism**: We record (1) the deviation of the closed-loop trajectory from the trajectory obtained without TVs: $\Delta\tau$, (2) the smallest Euclidean distance observed between the EV and TV: \bar{d}_{min} and (3) the

feasibility % of the SMPC optimization problem: \mathcal{F} . While an increase in (1) and (2) corresponds to higher safety, a large value could indicate an over-conservative planner and resulting low values of (3).

- **Computational Efficiency**: This is the average time taken by the solver: \bar{T}_{solve} ; lower is better.

V. RESULTS

In this section, we present the results of the various SMPC policies (Section IV-D). For each scenario, we deploy each policy for 4 different initial conditions by varying: (1) the starting distance from the intersection in $\{10 \text{ m}, 20 \text{ m}\}$ and (2) the initial speed in $\{8 \text{ m s}^{-1}, 10 \text{ m s}^{-1}\}$. For all the policies, we use a prediction horizon of $N = 10$, discretization time-step for the EV dynamics as $dt = 0.2 \text{ s}$, and a risk level of $\epsilon = 0.05$ for the chance constraints.

The closed-loop performance metrics, averaged across the initial conditions, are shown in Table I. **SMPC** is able to improve or maintain mobility compared to the baselines. There is a noticeable improvement in comfort and conservatism metrics, as the **SMPC** can stay close to the TV-free reference trajectory without incurring high acceleration/jerk or getting too close to the TVs. Finally, while the **SMPC_OL** ablation is the fastest in solve time, the **SMPC** can be used real-time at approximately 20 Hz. These results highlight the benefits of our SMPC in closed-loop execution.

VI. CONCLUSION

We proposed a SMPC formulation for EV control at traffic intersections, which uses GMMs for predicting TV trajectories for collision avoidance chance-constraints. The SMPC optimizes over a novel class of policies parameterised as a SOC, given by the sum of affine disturbance feedback over the EV’s states and linear state feedback over the TV’s states. By exploiting additional structure in the GMM predictions, the proposed policy class is TV mode-agnostic for the first $\bar{k} - 1$ time steps in the SMPC prediction horizon, and has separate mode-dependent policies for the remainder. The resulting SMPC optimization problem was shown to be a SOCP, which can be solved reliably and at approximately 20 Hz. Evaluating our algorithm against open-loop baselines along axes of mobility, comfort, conservatism and computational efficiency, we observed gains in mobility, comfort and efficiency while remaining significantly less conservative.

REFERENCES

- [1] N. H. T. S. Administration, "Automated vehicles for safety," <https://www.nhtsa.gov/technology-innovation/automated-vehicles-safety>, 2020.
- [2] —, "Crash factors in intersection-related crashes: An on-scene perspective," <http://www.nrd.nhtsa.dot.gov/Pubs/811366.pdf>, 2010.
- [3] L. Wei, Z. Li, J. Gong, C. Gong, and J. Li, "Autonomous driving strategies at intersections: Scenarios, state-of-the-art, and future outlooks," *arXiv preprint arXiv:2106.13052*, 2021.
- [4] H. A. P. Blom and Y. Bar-Shalom, "The interacting multiple model algorithm for systems with markovian switching coefficients," *IEEE Transactions on Automatic Control*, vol. 33, no. 8, pp. 780–783, 1988.
- [5] Y. Chai, B. Sapp, M. Bansal, and D. Anguelov, "Multipath: Multiple probabilistic anchor trajectory hypotheses for behavior prediction," *arXiv preprint arXiv:1910.05449*, 2019.
- [6] T. Salzmann, B. Ivanovic, P. Chakravarty, and M. Pavone, "Trajectron++: Dynamically-feasible trajectory forecasting with heterogeneous data," in *Computer Vision—ECCV 2020: 16th European Conference, Glasgow, UK, August 23–28, 2020, Proceedings, Part XVIII 16*. Springer, 2020, pp. 683–700.
- [7] M. Morari and J. H. Lee, "Model predictive control: past, present and future," *Computers & Chemical Engineering*, vol. 23, no. 4-5, pp. 667–682, 1999.
- [8] B. Recht, "What we've learned to control," <https://www.argmin.net/2020/06/29/tour-revisited/>, 2020.
- [9] W. Schwarting, J. Alonso-Mora, and D. Rus, "Planning and decision-making for autonomous vehicles," *Annual Review of Control, Robotics, and Autonomous Systems*, vol. 1, no. 1, pp. 187–210, 2018.
- [10] U. Rosolia, X. Zhang, and F. Borrelli, "Data-driven predictive control for autonomous systems," *Annual Review of Control, Robotics, and Autonomous Systems*, vol. 1, pp. 259–286, 2018.
- [11] A. Mesbah, "Stochastic model predictive control: An overview and perspectives for future research," *IEEE Control Systems Magazine*, vol. 36, no. 6, pp. 30–44, 2016.
- [12] A. Carvalho, Y. Gao, S. Lefevre, and F. Borrelli, "Stochastic predictive control of autonomous vehicles in uncertain environments," in *12th International Symposium on Advanced Vehicle Control*, 2014, pp. 712–719.
- [13] A. Gray, Y. Gao, T. Lin, J. K. Hedrick, and F. Borrelli, "Stochastic predictive control for semi-autonomous vehicles with an uncertain driver model," in *16th International IEEE Conference on Intelligent Transportation Systems (ITSC 2013)*. IEEE, 2013, pp. 2329–2334.
- [14] D. Moser, R. Schmied, H. Waschl, and L. del Re, "Flexible spacing adaptive cruise control using stochastic model predictive control," *IEEE Transactions on Control Systems Technology*, vol. 26, no. 1, pp. 114–127, 2017.
- [15] V. Causevic, Y. Fanger, T. Brüdigam, and S. Hirche, "Information-constrained model predictive control with application to vehicle platooning," *IFAC-PapersOnLine*, vol. 53, no. 2, pp. 3124–3130, 2020.
- [16] B. Zhou, W. Schwarting, D. Rus, and J. Alonso-Mora, "Joint multi-policy behavior estimation and receding-horizon trajectory planning for automated urban driving," in *2018 IEEE International Conference on Robotics and Automation (ICRA)*. IEEE, 2018, pp. 2388–2394.
- [17] A. Wang, A. Jasour, and B. C. Williams, "Non-gaussian chance-constrained trajectory planning for autonomous vehicles under agent uncertainty," *IEEE Robotics and Automation Letters*, vol. 5, no. 4, pp. 6041–6048, 2020.
- [18] P. J. Goulart, E. C. Kerrigan, and J. M. Maciejowski, "Optimization over state feedback policies for robust control with constraints," *Automatica*, vol. 42, no. 4, pp. 523–533, 2006.
- [19] G. Schildbach, M. Soppert, and F. Borrelli, "A collision avoidance system at intersections using robust model predictive control," in *2016 IEEE Intelligent Vehicles Symposium (IV)*. IEEE, 2016, pp. 233–238.
- [20] I. Batkovic, U. Rosolia, M. Zanon, and P. Falcone, "A robust scenario mpc approach for uncertain multi-modal obstacles," *IEEE Control Systems Letters*, vol. 5, no. 3, pp. 947–952, 2020.
- [21] J. Kong, M. Pfeiffer, G. Schildbach, and F. Borrelli, "Kinematic and dynamic vehicle models for autonomous driving control design," in *2015 IEEE Intelligent Vehicles Symposium (IV)*. IEEE, 2015, pp. 1094–1099.
- [22] A. Dosovitskiy, G. Ros, F. Codevilla, A. Lopez, and V. Koltun, "CARLA: An open urban driving simulator," in *Proceedings of the 1st Annual Conference on Robot Learning*, 2017, pp. 1–16.

- [23] J. Houston, G. Zuidhof, L. Bergamini, Y. Ye, A. Jain, S. Omari, V. Igloukov, and P. Ondruska, "One thousand and one hours: Self-driving motion prediction dataset," 2020.
- [24] A. Wächter and L. T. Biegler, "On the implementation of an interior-point filter line-search algorithm for large-scale nonlinear programming," *Mathematical programming*, vol. 106, no. 1, pp. 25–57, 2006.
- [25] Gurobi Optimization, LLC, "Gurobi Optimizer Reference Manual," 2021. [Online]. Available: <https://www.gurobi.com>

APPENDIX

A. Matrix definitions

$$\mathbf{h}_t^j = [h_{0|t}^\top \dots h_{\bar{k}-1|t}^\top h_{\bar{k}|t}^\top \dots h_{N-1|t}^\top]^\top$$

$$\mathbf{K}_t^j = \text{blkdiag} \left(K_{0|t}, \dots, K_{\bar{k}-1|t}, K_{\bar{k}|t}^j, \dots, K_{N-1|t}^j \right)$$

$$\mathbf{M}_t^j = \begin{bmatrix} O & \dots & \dots & \dots & O \\ M_{0,1|t} & O & \dots & \dots & O \\ \vdots & \vdots & \vdots & \vdots & \vdots \\ M_{0,\bar{k}-1|t} & \dots & M_{\bar{k}-2,\bar{k}-1|t} & O & \dots & O \\ M_{0,\bar{k}|t}^j & \dots & \dots & M_{\bar{k}-1,\bar{k}|t}^j & \dots & O \\ \vdots & \vdots & \vdots & \vdots & \vdots & \vdots \\ M_{0,N-1|t}^j & \dots & \dots & \dots & M_{N-2,N-1|t}^j & O \end{bmatrix}$$

$$\mathbf{A}_t = \begin{bmatrix} I_4 \\ A_{0|t} \\ A_{1|t} A_{0|t} \\ \vdots \\ \prod_{k=0}^{N-1} A_{k|t} \end{bmatrix}, \mathbf{B}_t = \begin{bmatrix} O & \dots & \dots & O \\ B_{0|t} & O & \dots & O \\ A_{1|t} B_{0|t} & B_{1|t} & \dots & O \\ \vdots & \ddots & \ddots & \vdots \\ \prod_{k=1}^{N-1} A_{k|t} B_{0|t} & \dots & \dots & B_{N-1|t} \end{bmatrix},$$

$$\mathbf{T}_t^j = \begin{bmatrix} I_2 \\ T_{0|t,j} \\ T_{1|t,j} T_{0|t,j} \\ \vdots \\ \prod_{k=0}^{N-1} T_{k|t,j} \end{bmatrix}, \mathbf{C}_t^j = \begin{bmatrix} O \\ c_{0|t,j} \\ c_{1|t,j} + T_{1|t,j} c_{0|t,j} \\ \vdots \\ c_{N-1|t,j} + \sum_{k=0}^{N-1} \prod_{l=k+1}^{N-1} T_{l|t,j} c_{k|t,j} \end{bmatrix}$$

$$\mathbf{E}_t = \begin{bmatrix} O & \dots & \dots & O \\ I_4 & O & \dots & O \\ A_{1|t} & I_4 & \dots & O \\ \vdots & \ddots & \ddots & \vdots \\ \prod_{k=1}^{N-1} A_{k|t} & \dots & \dots & I_4 \end{bmatrix}, \mathbf{L}_t^j = \begin{bmatrix} O & \dots & \dots & O \\ I_2 & O & \dots & O \\ T_{1|t,j} & I_2 & \dots & O \\ \vdots & \ddots & \ddots & \vdots \\ \prod_{k=1}^{N-1} T_{k|t,j} & \dots & \dots & I_2 \end{bmatrix}$$

$$\mathbf{Q} = I_{N+1} \otimes Q, \mathbf{R} = I_N \otimes R, \Sigma_w = I_N \otimes \Sigma_w, \Sigma_n = I_N \otimes \Sigma_n$$

B. Proof of proposition 1

Defining $n_{k|t,j} \sim \mathcal{N}(0, \bar{\Sigma}_{k+1|t,j}) \forall k \in \mathcal{I}_0^{N-1}$, we can use the closure of Gaussian random variables under linear combinations and the orthogonality principle, to rewrite (8) as $o_{k+1|t,j} = T_{k|t,j} o_{k|t,j} + c_{k|t,j} + n_{k|t,j}$. Thus

$$\begin{aligned} o_{k|t,j} &= \prod_{l=0}^{k-1} T_{l|t,j} o_t + \sum_{m=0}^{k-1} \prod_{l=m}^{k-2} T_{l+1|t,j} (c_{m|t,j} + n_{m|t,j}) \\ &= \sqrt{\Sigma_{k|t,j}} \sqrt{\Sigma_{1|t,j}^{-1}} o_t + \mu_{k|t,j} - \sqrt{\Sigma_{k|t,j}} \sqrt{\Sigma_{k-1|t,j}^{-1}} \mu_{k-1|t,j} \\ &\quad + \sqrt{\Sigma_{k|t,j}} \sqrt{\Sigma_{k-1|t,j}^{-1}} \mu_{k-1|t,j} - \sqrt{\Sigma_{k|t,j}} \sqrt{\Sigma_{k-2|t,j}^{-1}} \mu_{k-2|t,j} \dots \\ &\quad - \sqrt{\Sigma_{k|t,j}} \sqrt{\Sigma_{1|t,j}^{-1}} o_t + n_{k-1|t,j} + \sum_{m=0}^{k-2} \prod_{l=m}^{k-2} T_{l+1|t,j} n_{m|t,j} \\ &= \mu_{k|t,j} + n_{k-1|t,j} + \sqrt{\Sigma_{k|t,j}} \sqrt{\Sigma_{1|t,j}^{-1}} n_{0|t,j} \\ &\quad + \sum_{m=1}^{k-2} \prod_{l=m}^{k-2} \sqrt{\Sigma_{k-1|t,j}} \sqrt{\Sigma_{m|t,j}^{-1}} n_{m|t,j} \end{aligned}$$

